Influence of Position Isomerism on the Chiral Properties in Sequence-Defined Conjugated Macromolecules

Influence of position isomerism on the chiral properties in sequence-defined conjugated macromolecules

Wout Milis[a], *Ginevra Calzolai*[a,b], *Elisabetta Salatelli*[b], *Guy Koeckelberghs*[a]*

Laboratory for Polymer Synthesis, KU Leuven, Celestijnenlaan 200F – box 2404, B-30001, Heverlee, Belgium. [a]

Department of Industrial Chemistry "Toso Montanari", University of Bologna, Viale Risorgimento 4, 40136 Bologna, Italy.[b]

For Table of Contents use only

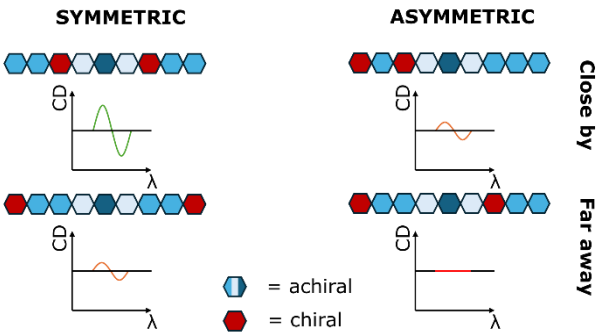

KEYWORDS: Conjugated polymers, sequence-defined, circular dichroism, position isomers, chirality, asymmetry, symmetry.

Abstract

The chiral expression in conjugated polymers (CPs) has garnered significant attention, particularly due to its dependence on the aggregation process. Many variables that influence the chiral response have been investigated, however, achieving absolute control over the primary structure remains challenging. In this study, an orthogonal approach is used to develop sequence-defined conjugated macromolecules with precisely control over monomer sequence and primary structure. The influence of position isomers is investigated by synthesizing four enantiomeric co-oligomers, composed of two chiral monomers out of nine. Solvatochromism experiments, using UV-vis and circular dichroism (CD) experiments, are conducted to examine the chiroptical response. This study investigates not only the monomer position but also the role of (a)symmetry along with the concentration dependence, to determine whether an inter- or intramolecular process occurs. These findings provide valuable insights into controlling the chiroptical properties of CPs, paving the way for improved material design for optoelectronic applications.

Introduction

Chirality is a fundamental characteristic of many natural and synthetic systems, playing a crucial role in the functioning of active pharmaceutical ingredients and biological polymers. The influence of chirality on the properties of these compounds is pivotal to their potential applications. For instance, chirality plays a major role in the quality and intensity of flavors and fragrances, but also impacts the quaternary structure and thus catalytic function of enzymes. While the effects of chirality on biological polymers are well recognized, its impact on synthetic polymers, such as polyisocyanates, is equally significant. Combinations of chiral and achiral monomers, or chiral monomers with opposite handedness, result in chirality amplification due to cooperative effects, known as the sergeant-and-soldiers and majority rules principles,

respectively.[1,2] An other compelling class of polymers where this cooperative effect of chirality is observed, is in conjugated polymers (CPs).[3]

The last decades, CPs have emerged as an essential class of materials that exhibit unique optoelectronic properties, making them suitable for a wide range of applications, including organic photovoltaics (oPVs),[4–6] organic field-effect transistors (oFETs),[7–9] organic light-emitting diodes (oLEDs),[8,10] drug delivery systems,[11] thermo-electrics (TE),[12,13] chemical sensors[14] and many more. The performance of these devices is intrinsically linked to the structural characteristics of the polymer backbone, such as chain length, monomer sequence, functional end groups, and structural defects.[15,16] These factors directly affect the highest occupied molecular orbital (HOMO) and lowest unoccupied molecular orbital (LUMO) levels, but also the overall supramolecular organization.[17] Consequently, precise control over these parameters is crucial for the development of reproducible, high-performance materials.[18,19]

Among the various investigated properties of CPs, chiral expression has garnered significant attention, particularly due to its dependence on the aggregation process.[20,21] Chirality in CPs is commonly introduced through monomers with a stereogenic carbon atom in their sidechains, leading to the formation of inter- or intramolecular helical structures rather than conventional lamellar arrangements. As mentioned earlier, the properties of CPs are affected by many parameters and the same holds for the chiral properties. Besides the type and number of chiral monomers applied in homo- and copolymers,[22,23] the chirality is also effected by the nature and position of structural defects in the backbone,[24,25] end group variations[26] as well as the dispersity.[27] Despite the advancements in understanding these parameters, achieving absolute control over the chiral aggregation of CPs remains challenging. Inherently associated with the traditional polymerization techniques, for both conjugated homo- and copolymers, is the

variation in chain length, dispersity, lack of control over end groups, and undefined monomer sequences.

To address these limitations, scientists have drawn inspiration from well-known biopolymers, such as DNA and proteins, which exhibit the remarkable ability of precise control over monomer sequence and structure. This level of control was first synthetically replicated by Merrifield and marked the advent of sequence-defined polymers, enabling the specific incorporation of monomers at predetermined positions within the polymer backbone to finetune the properties at will.[28] Ever since, many approaches have been developed following mainly two methodologies. One approach follows the pattern of Merrifield, using activation/deactivation syntheses, requiring two steps per chain elongation, [29–35] while the other is based on orthogonal reactions where each step introduces a new monomer into the polymer backbone.[36–40]

In the context of CPs, our group recently introduced a versatile orthogonal synthesis strategy that enables precise incorporation of monomers at designated positions along the backbone.[41] This method allows for the controlled synthesis of sequence-defined conjugated macromolecules, but also controls the functional end groups, facilitating post-polymerization modifications and enabling the linkage of oligomer chains to various (macro)molecules. This strategy significantly broadens the functional scope and potential applications of these materials.

In this study, we employ this orthogonal sequence-defined approach to precisely incorporate chiral monomers at specific positions within the oligomer backbone. This method not only enables control over the primary monomer sequence and functional end groups, but also over structural defects, dispersity, and chain length, facilitating a comprehensive structure-property analysis. As a result, the properties are only influenced by the sequence of chiral monomers and offer new insights into the chiral aggregation of conjugated macromolecules. To explore these

effects, four different nonamers are developed and their chiral aggregation is investigated employing circular dichroism (CD) spectroscopy. These four macromolecules are composed of an equal number of chiral and achiral monomers within the backbone, creating distinct isomeric structures with varying proximities of the chiral monomers (figure 1). Additionally, the impact of (a)symmetry is examined by comparing symmetrical and asymmetrical structures centered around a core molecule. Finally, the nature of aggregate formation, whether it is an inter- or intramolecular process, is investigated through analyzing the concentration dependence of the aggregation behavior.

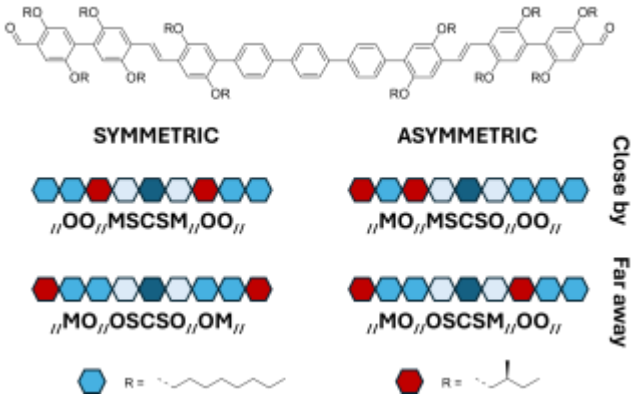

Figure 1. Schematic overview of the four enantiomeric oligomers with the backbone shown on top. On the left side are the symmetric oligomers illustrated, and on the right side the asymmetric sequences. **O** denotes a monomer with an octyl side chain, while **M** denotes a monomer with a *S*-chiral methylbutyl side chain. The // in the codenames illustrate where the double bond/aldehyde functions can be found.

Results and discussion

Synthesis

Orthogonal sequence-defined macromolecules are synthesized using two different types of monomers, one *AB* functionalized monomer and one *CD* functionalized monomer. To ensure

selective elongation of the macromolecule, it is important that function *A* only reacts with function *C,* while function *B* exclusively reacts with function *D*. Recently, our group developed an orthogonal approach towards sequence-defined conjugated macromolecules based on the Suzuki-Miyaura cross coupling (SMCC) and the Horner-Wadsworth-Emmons (HWE) reaction.[42–44] The functional groups used are a boronic ester (*A*) and aryl bromide (*C*) for the SMCC and an aldehyde (*B*) and phosphonate (*D*) in the HWE reaction. To establish unidirectional growth of the macromolecule, a starting monomer (**S**) is used with only one of the four reactive functionalities, namely the aryl bromide (*C*) (figure 2A). Additionally, this molecule also possesses a (protected) hydroxyl group required for post polymerization reactions, as will be discussed later.

The appropriate monomers are synthesized as described in literature and their synthesis starts from the widely available hydroquinone (Figure S1). In the first step, the hydroquinone is subjected to a Williamson ether synthesis to introduce either achiral *n*-octyl sidechains or chiral (*S*)-2-methylbutyl sidechains (O and M monomers, respectively, figure 2B). This is followed by a dibromination and a Bouveault reaction, introducing a bromide and aldehyde function in *para*-position. This specific aldehyde compound serves as a mutual intermediate to synthesize the required monomers. On one hand, the bromide is converted to a boronic ester via a Miyaura borylation, resulting in a phenyl monomer equipped with an aldehyde and boronic ester function (**O**// and **M**//). On the other hand, the aldehyde is reduced to an alcohol, followed by a chlorination reaction and subjected to the Arbuzov reaction to obtain the required phosphonate-bromide monomer (**O**).

A)

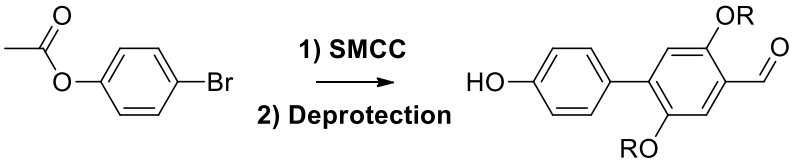

S

B)

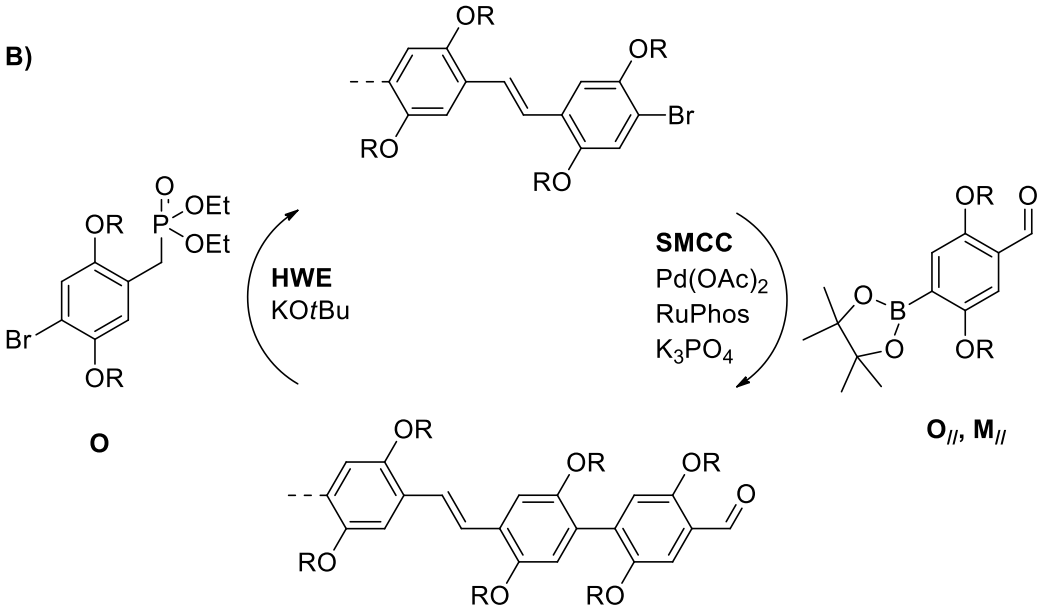

O

O//, M//

C)

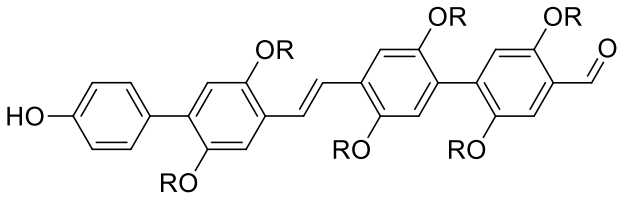

SO//OO//
SM//OO//
SO//OM//
SM//OM//

O//, O =

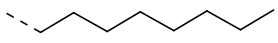

M// =

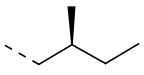

Figure 2. A) First SMCC reaction with starting molecule **S** with a protected alcohol function. After the coupling reaction, the alcohol is deprotected. B) Overview of the orthogonal reactions and monomers. C) Illustration of the backbone of the four distinct tetramers. In all codings, **S** represents the starting molecules, **O** refers to a monomer with an octyl side chain, while **M** denotes a *S*-chiral methylbutyl side chain. The // illustrate where the double bond/aldehyde functions can be found.

In order to study the effect of the chiral monomer position and the (a)symmetry effect on the chiral properties, four distinct nonamers are developed. The nonamers are synthesized from two tetramers, which are synthesized orthogonally, and coupled onto a central core molecule (**C**). The symmetrical structures are easily obtained by reacting two equivalents of the same tetramer with only one equivalent of the central core. The asymmetrical nonamers are, obviously, synthesized in two steps. First, one tetramer is reacted with the central core molecule, followed by the addition of a different tetramer in a second step. All four nonamers consist of an equal number of chiral monomers, namely two, resulting in four enantiomeric co-oligomers.

The four distinct oligomers, **SO//OO//**, **SM//OO//**, **SO//OM//**, and **SM//OM//**, are synthesized iteratively starting from molecule **S** and their backbone is illustrated in Figure 2C. Note that the hydroxyl group is protected as an acetate in the first SMCC, which is required to prevent solubility issues and improves reaction rates. After the first coupling reaction, the acetate group is no longer recommended and the alcohol function is deprotected to avoid unwanted side reactions with KO*t*Bu in subsequent HWE reactions.

After the tetramer synthesis, the oligomer chains possess an alcohol and aldehyde function at both oligomer chain ends. The alcohol function is used in a post-polymerization reaction to convert to a triflate function (pseudohalogen), making it susceptible to cross coupling reactions

with other (macro)molecules. Instead of using the more harmful and reactive triflic anhydride, this conversion is performed with milder and easier to handle di(trifluoromethanesulfonyl)aniline and is catalyzed by DMAP (Figure S12).

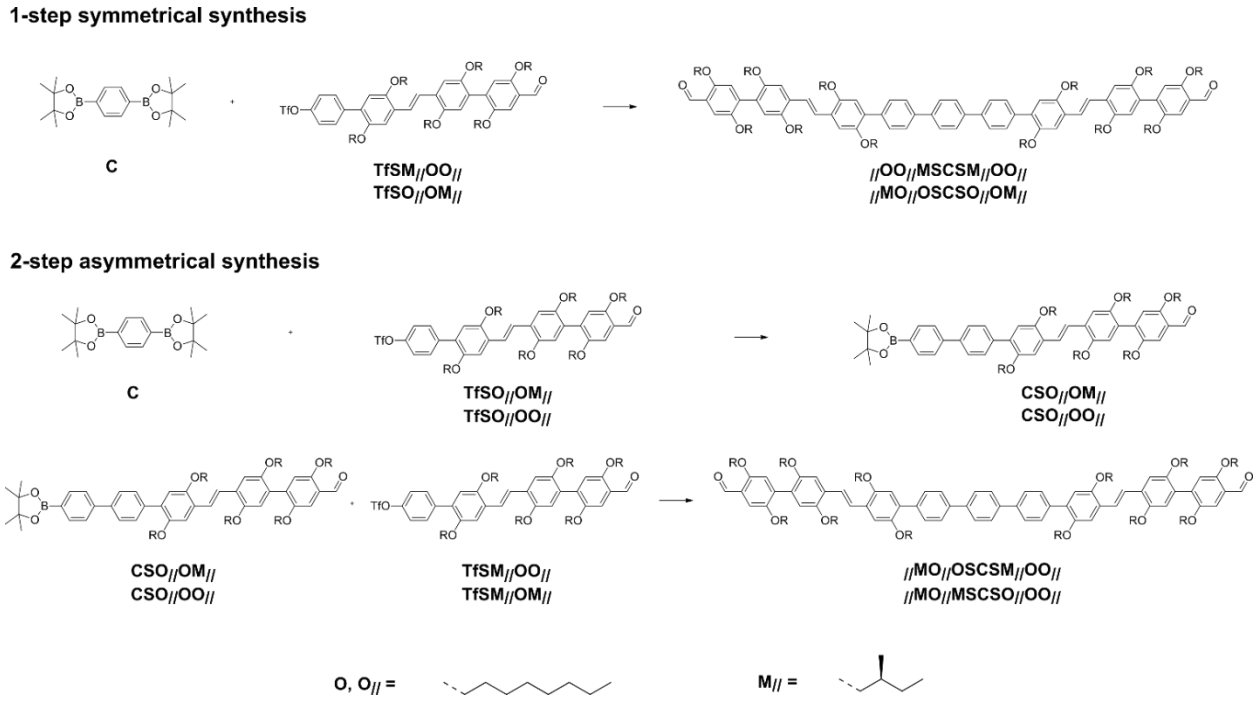

Figure 3. Overview of the synthesis of both the symmetrical and asymmetrical nonamers.

The symmetrical nonamers (//**MO**//**OSCSO**//**OM**// and //**OO**//**MSCSM**//**OO**//) are easily developed using a small excess of the respective tetramers (2.2 equivalents) relative to the central core molecule, 1,4-benzenediboronic acid bis(pinacol) ester (**C**) (figure 3). The asymmetrical sequences are synthesized in a two step process and to prevent the formation of symmetrical nonamers, a 10-fold excess of **C** is reacted with **TfSO**//**OO**// or **TfSO**//**OM**// to synthesize intermediate products **CSO**//**OO**// and **CSO**//**OM**//. To further diminish the possibility of a double coupling on a single core molecule, the tetramer is added dropwise over a 10 min timespan via an automated syringe pump. Despite these precautions, the symmetrical product was still observed. Instead of working on a 0.2-0.1 M concentration relative to the oligomer,

working with the same concentration relative to the core molecule (10 times dilution) did not result in any improved selectivity of mono reacted versus double reacted products (Figure S13). The synthesized pentamer might be too electron rich, making it amenable for the Pd catalyst to stay complexed to the macromolecule, favoring a second reaction.[45] Due to this inconvenience, the purification by column chromatography or crystallization/precipitation was severely hindered as both products (the single and double reacted) were hardly separatable via column chromatography and inseparable with crystallization or precipitation techniques. Additionally, the instability of boronic esters on the (acidic) silica used for column chromatography resulted in low yields. Alternative stationary phases such as basic silica and neutral alumina did not work either. Fortunately, we managed to purify the oligomers by using preparative recycling size exclusion chromatography (SEC) (Figure S15).

In the last step, **CSO//OO//** and **CSO//OM//** are reacted with **TfSM//OM//** and **TfSM//OO//**, respectively, to obtain the asymmetrical nonamers, both with an equal number of chiral monomers in the backbone. The coupling is monitored by ^{1}H NMR by the disappearance of the doublet signal of end standing phenyl ring (Figure S14). A moderate excess of 1.2 equivalents of the triflate oligomers is used for complete conversion and the excess is removed via crystallization in order to obtain the pure asymmetrical nonamers **//MO//MSCSO//OO//** and **//MO//OSCSM//OO//**.

Chiroptical properties

Before analyzing the aggregation and corresponding chiral response, it is verified that all other parameters influencing the electronic properties are consistent, with the monomer sequence being the only variable. Therefore, UV-vis and fluorescence measurements are conducted on the four different nonamers. When all parameters that influence the electronic properties are

identical, the optical results of all four nonamers should be equivalent. As shown in Figure 4, the UV-vis and fluorescence spectra are clearly very similar. The extinction coefficient for the four nonamers are ranging from 42.4 ($L \cdot g^{-1} \cdot cm^{-1}$) for //**MO**//**MSCSO**//**OO**// to 49.6 ($L \cdot g^{-1} \cdot cm^{-1}$) for //**MO**//**OSCSM**//**OO**//, which falls within the experimental weighing error**.** Additionally, the λ_{max} for all four oligomers is consistently located at 396 nm. The fluorescence data, normalized by the absorbance of excitation to obtain concentration independent results, further confirms the electronic similarities between the nonamers. Again, the intensities are in the same range with the wavelength of maximum fluorescence located at 505-506 nm for all oligomers.

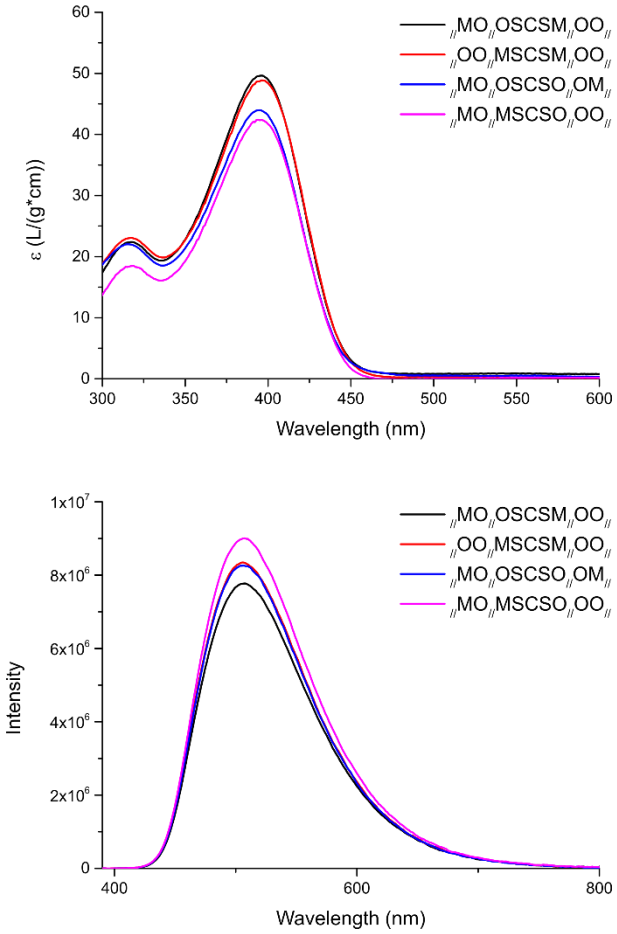

Figure 4. UV-vis (top) and fluorescence (bottom) spectra of the four nonamers. The fluorescence data is divided by the absorbance of excitation to make the results concentration independent.

In order to investigate the chiral aggregation of the four different nonamers, solvatochromism experiments are conducted using UV-vis and CD spectroscopy. Starting from a solution in a good solvent, solutions with increasing concentrations of nonsolvent are step-by-step established to induce aggregation of the oligomers. The nonamers are dissolved in chloroform ($CHCl_3$) as a good solvent, while methanol (MeOH) is used as nonsolvent. The addition of nonsolvent reduces the solubility of the oligomers, amplifying the π-π interactions of the oligomer backbones. Due

to the chiral side chains, this aggregation may not occur in a lamellar fashion, but a (moderate) twist between consecutive chains or intramolecular chiral conformations may be formed.

In a series of a single nonamer, the concentration of the oligomer is maintained, while the ratio of good solvent over nonsolvent is gradually changed. The solution of good solvent and oligomer is stirred at 400 RPM while the nonsolvent is added at a rate of 100 μL/min by using an automatic syringe pump. Immediately after addition, the UV-vis measurements followed by the CD measurements are performed. The measurements are conducted in 2x10 mm quartz cuvettes (Figure 5).

SYMMETRIC

ASYMMETRIC

Far away

Close by

Close by

Far away

//MO//OSCSO//OM//

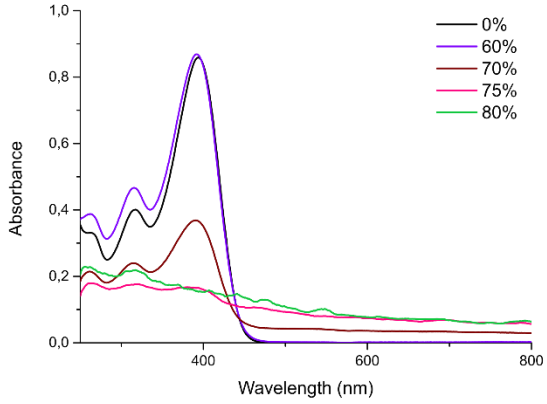

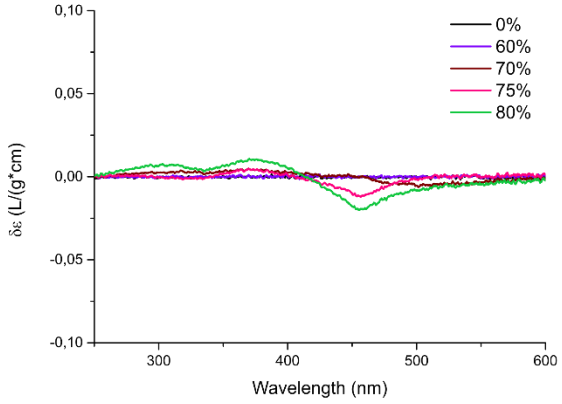

//OO//MSCSM//OO//

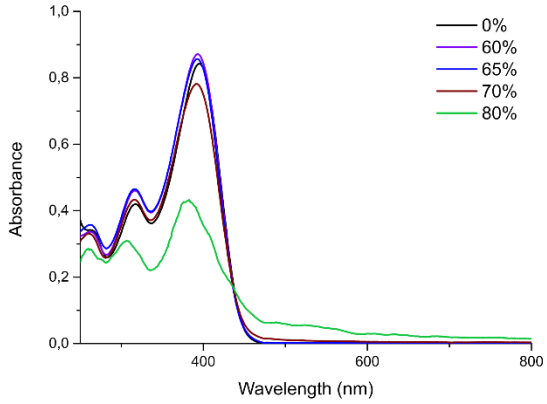

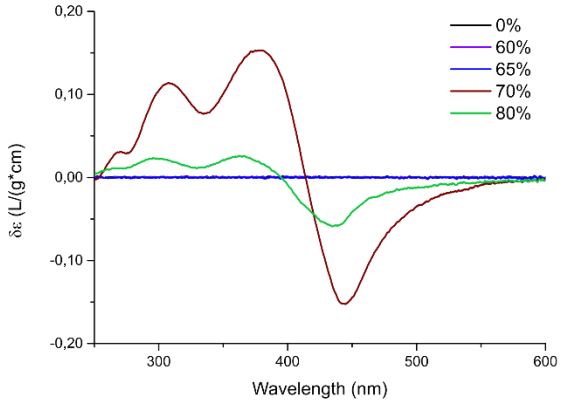

//MO//MSCSO//OO//

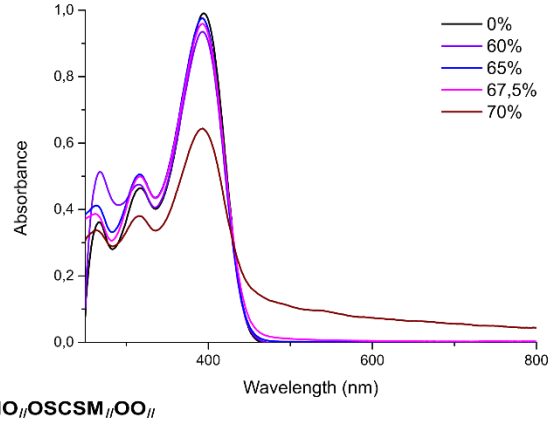

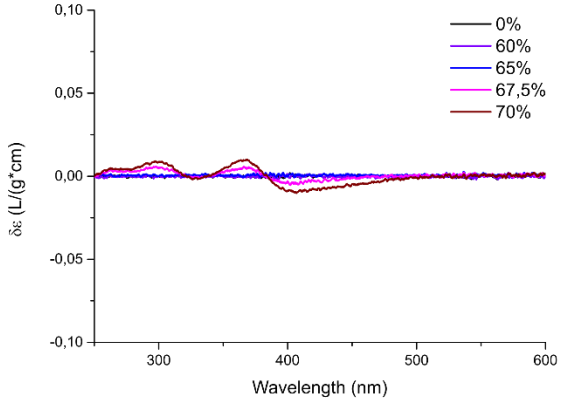

//MO//OSCSM//OO//

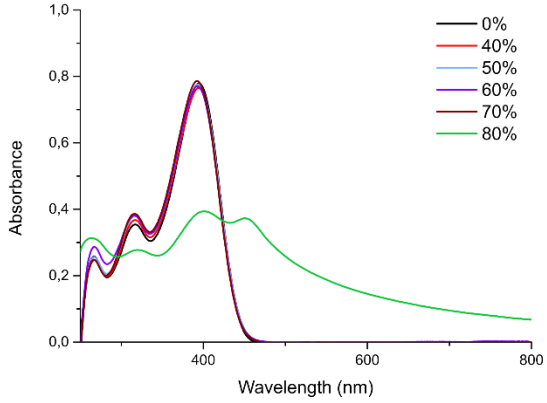

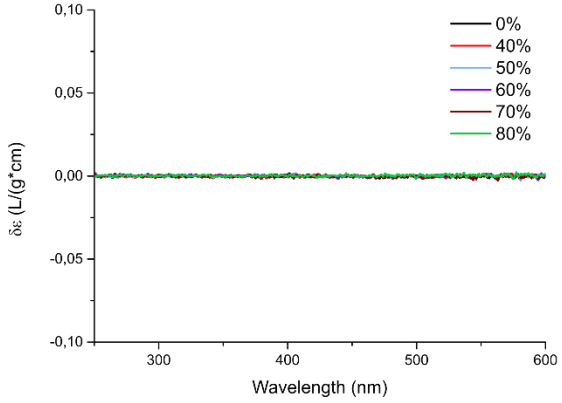

Figure 5. UV-vis (left) and CD (right) spectra of the four nonamers. On top the symmetric sequences //**MO**//**OSCSO**//**OM**// and //**OO**//**MSCSM**//**OO**//, and below the asymmetric sequences, //**MO**//**MSCSO**//**OO**// and //**MO**//**OSCSM**//**OO**//. In the legend, the quantity of nonsolvent is given (MeOH).

Upon the addition of nonsolvent, the oligomers tend to aggregate and planarize due to more favorable π-π interactions, which is often manifested by a redshift of the λ_{max} signal in UV-vis spectroscopy. However, among the four nonamers investigated, this redshift is observed only in a few conditions involving the asymmetrical sequences (//**MO**//**OSCSM**//**OO**// 80 % MeOH and SI S41), while this is absent in all symmetrical ones. Although a redshift is absent in many spectra, aggregate formation is evidenced by the scattering observed in the higher wavelength region (500 – 800 nm), along with a decrease in intensity of the λ_{max} signal. The overall similarities of the UV-vis spectra across all sequences implies that, aside from the aggregate formations, the supramolecular organization is also similar. If clear differences in the spectra would be observed, such as varying λ_{max} or shape of the spectrum, this would indicate the formation of different supramolecular structures.

Similar as in the UV-vis spectra, all CD spectra indicating chiral aggregation are consistent and characterized by two clear signals. Remarkably, the sign of the signal is the same in all nonamers. The negative bisignate signal with zero crossing near 400 nm, corresponds to the UV-vis absorption at 396 nm and originates from the backbone of the chirally stacked oligomers. The second, monosignate CD signal at lower wavelength (~300 nm), corresponds to the UV-vis signal at ± 325 nm and represents an interaction perpendicular to the oligomer main chain.

While the shape of the chirally active sequences is identical, clear distinctions are observed in the intensity of the CD spectra. Both symmetric sequences show clear signs of chiral expression; //**OO**//**MSCSM**//**OO**// exhibits a significantly more intense CD signal compared with //**MO**//**OSCSO**//**OM**//, though the sign, and therefore the handedness of the helicity is identical.

This is a remarkable observation as the corresponding tetramers (**SO**//**OM**//and **SM**//**OO**//) display a reversed difference in intensity and with opposite signs (Figure S19).[41] In the asymmetrical sequences, //**MO**//**OSCSM**//**OO**// did not show any chirality, while //**MO**//**MSCSO**//**OO**// is similar to the spectrum of //**MO**//**OSCSO**//**OM**//. Note that the sequences studied are intrinsically co-oligomers with only a minimal number of chiral monomers (22 %) in the backbone contributing to their chiral behavior.

Based on these findings, guidelines towards macromolecules with enhanced chiral properties can be established. First, it is clear that symmetry enhances the ability to aggregate in a chiral fashion, whereas asymmetry appears to be disadvantageous. Additionally, placing the chiral monomers closer to each other also improves the chiral aggregation as evidenced by stronger chiral expression in //**OO**//**MSCSM**//**OO**// versus //**MO**//**OSCSO**//**OM**// in the symmetrical oligomers, and //**MO**//**MSCSO**//**OO**// versus //**MO**//**OSCSM**//**OO**// in the asymmetrical oligomers. Although scattering due to aggregation is observed in the UV-vis spectra, it did not influence the CD signals as no clear deviations are observed in the higher wavelength region (500 – 600 nm). However, these aggregates might have caused less intense CD signals due to lower concentrations of oligomers.

The assembly of the chiral aggregates can potentially arise from two different origins. On one hand, the presence of the planar stilbene moieties can be a driving force to form (helical) stacks. On the other hand, the twisted and unsubstituted *p*-terphenyl structure in the center of the nonamer can drive it toward an intramolecular helical conformation. The difference between these two processes is investigated by performing solvatochromism experiments with varying oligomer concentrations (Figure 6). If the chiral response is found to be concentration independent, this would demonstrate the formation of intramolecular helices and vice versa.

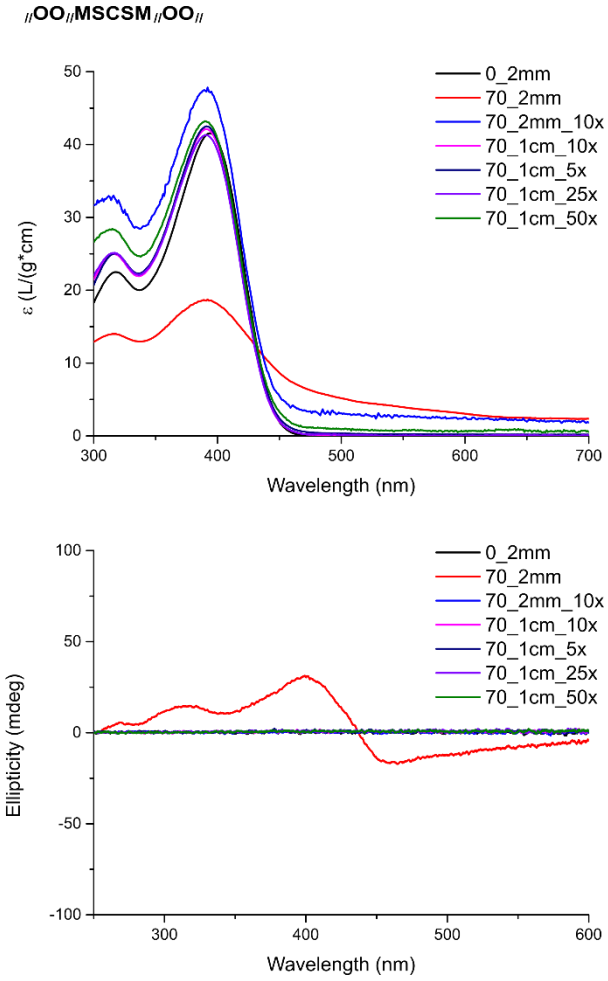

Figure 6. UV-vis (top) and CD (bottom) spectra of the concentration dependence experiment with //**OO**//**MSCSM**//**OO**//. The legend follows the logic order of percentage of nonsolvent_cuvette dimensions_dilution factor.

For this purpose, the oligomer exhibiting the most pronounced chiral expression is used at concentrations similar as in the previous paragraph, with additional dilutions of factor 5, 10, 25, and 50. Analogous conditions are applied, meaning that $CHCl_3$ is used as good solvent again and MeOH as nonsolvent. The reference measurement is conducted in 2x10 mm quartz cuvettes, while the factor 5, 25 and 50 are performed in 10x10 mm quartz cuvettes. The factor 10 dilution is performed in both, 2x10 mm and 10x10 mm quartz cuvettes. Despite performing these dilutions, only the reference sample showed a CD signal, indicating that the chiral response is

concentration dependent. Consequently, the aggregation appears to be concentration dependent, demonstrating the formation of intermolecular helices.

Conclusion

This report investigates the chiroptical properties of four isomeric nonamers, which are synthesized with a versatile and efficient approach for the synthesis of sequence-defined conjugated macromolecules. These nonamers are obtained via an orthogonal approach to first develop four different tetramers, which are coupled onto a core molecule in different combinations in a modular approach. This strategy enables to perform a decent structure-property analysis since all parameters influencing the electronic characteristics are constant, except the sequence of chiral and achiral monomers. The obtained results offer groundbreaking guidelines for synthesizing polymers, aiming for high chiroptical responses. The co-oligomers, which contain only a minimal number of chiral monomers (22 %), demonstrate that both positioning chiral monomers in close proximity and creating symmetry withing the backbone is beneficial for the chiral response. Furthermore, solvatochromism experiments with varying concentrations are conducted to investigate the process, revealing that it leads to intermolecular aggregates.

ASSOCIATED CONTENT

Supporting Information.

Materials, Instrumentation, monomer synthesis, oligomer synthesis, NMR spectra of new compounds, SEC elution graphs of new compounds, HRMS data of new compounds, additional UV-vis and CD spectra, UV-vis and fluorescence data of the new tetramer.

AUTHOR INFORMATION

Corresponding Author

Guy Koeckelberghs – guy.koeckelberghs@kuleuven.be - Laboratory for Polymer Synthesis, KU Leuven, Celestijnenlaan 200F, B-3001 Heverlee, Belgium.

Author Contributions

All authors have given approval to the final version of the manuscript. W.M and G.C. synthesized all the compounds, conducted the structural characterization studies, and performed all the optical measurements. J.W. executed and analyzed the Maldi-MS measurements. P.G. and E.S. provided critical feedback on the manuscript, and G.K. supervised the project.

Wout Milis data curation, formal analysis, investigation, supervision, conceptualization, writing – original draft; Ginevra Calzolai data curation, formal analysis, investigation, writing – review & editing; Guy Koeckelberghs, conceptualization, funding acquisition, project administration, supervision, writing – review & editing

Funding Sources

Notes

The authors declare no competing financial interest.

ACKNOWLEDGEMENT

We would like to thank Pascal Gerbaux and Julien De Winter of the University of Mons for performing HRMS measurements and providing critical feedback on the original draft.

This research was funded by the Fund for Scientific Research (FWO-Flanders, grant number G0C6623N)

ABBREVIATIONS

CP, conjugated polymers; oPVs, organic photovoltaics; oFETs, organic field-effect transistors; oLEDs organic light-emitting diodes; TE, thermos-electrics; HOMO, highest occupied molecular orbital; LUMO, lowest unoccupied molecular orbital; CD, circular dichroism; SMCC, Suzuki-Miyaura cross coupling; HWE, Horner-Wadsworth-Emmons; NMR, nuclear magnetic resonance; DMAP, 4-dimethylaminopyridine; SEC, size exclusion chromatography; UV-vis, ultraviolet – visible; $CHCl_3$, chloroform; MeOH, methanol; RPM, rounds per minute; mm, millimeter;

REFERENCES

(1) Green, M. M.; Reidy, M. P.; Johnson, R. J.; Darling, G.; O'Leary, D. J.; Willson, G. Macromolecular Stereochemistry: The Out-of-Proportion Influence of Optically Active Comonomers on the Conformational Characteristics of Polyisocyanates. The Sergeants and Soldiers Experiment. *Journal of the American Chemical Society* **1989**, *111* (16), 6452–6454. DOI:10.1021/ja00198a084.

(2) Green, M. M.; Garetz, B. A.; Munoz, B.; Chang, H. P.; Hoke, S.; Cooks, R. G. Majority Rules in the Copolymerization of Mirror Image Isomers. *Journal of the American Chemical Society*. American Chemical Society 1995, pp 4181–4182. DOI:10.1021/ja00119a039.

(3) Langeveld-Voss, B. M. W.; Waterval, R. J. M.; Janssen, R. A. J.; Meijer, E. W. Principles of `majority Rules' and `sergeants and Soldiers' Applied to the Aggregation of Optically

Active Polythiophenes: Evidence for a Multichain Phenomenon. *Macromolecules* **1999**, *32* (1), 227–230. DOI:10.1021/ma981349y.

(4) Facchetti, A. π-Conjugated Polymers for Organic Electronics and Photovoltaic Cell Applications. *Chemistry of Materials* **2011**, *23* (3), 733–758. DOI:10.1021/CM102419Z/ASSET/IMAGES/LARGE/CM-2010-02419Z_0017.JPEG.

(5) Coakley, K. M.; McGehee, M. D. Conjugated Polymer Photovoltaic Cells. *Chemistry of Materials* **2004**, *16* (23), 4533–4542. DOI:10.1021/CM049654N/ASSET/IMAGES/LARGE/CM049654NF00009.JPEG.

(6) Brabec, C. J.; Gowrisanker, S.; Halls, J. J. M.; Laird, D.; Jia, S.; Williams, S. P.; Brabec, [C J; Brabec, C. J.; Gowrisanker, S.; Laird, D.; Jia, S.; Williams, S. P.; Halls, J. J. M. Polymer–Fullerene Bulk-Heterojunction Solar Cells. *Advanced Materials* **2010**, *22* (34), 3839–3856. DOI:10.1002/ADMA.200903697.

(7) Wang, C.; Dong, H.; Hu, W.; Liu, Y.; Zhu, D. Semiconducting π-Conjugated Systems in Field-Effect Transistors: A Material Odyssey of Organic Electronics. *Chemical Reviews* **2012**, *112* (4), 2208–2267. DOI:10.1021/CR100380Z.

(8) Sirringhaus, H. 25th Anniversary Article: Organic Field-Effect Transistors: The Path Beyond Amorphous Silicon. *Advanced Materials* **2014**, *26* (9), 1319–1335. DOI:10.1002/ADMA.201304346.

(9) Allard, S.; Forster, M.; Souharce, B.; Thiem, H.; Scherf, U. Organic Semiconductors for Solution-Processable Field-Effect Transistors (OFETs). *Angewandte Chemie International Edition* **2008**, *47* (22), 4070–4098. DOI:10.1002/ANIE.200701920.

(10) Wei, Q.; Ge, Z.; Voit, B. Thermally Activated Delayed Fluorescent Polymers: Structures, Properties, and Applications in OLED Devices. *Macromolecular Rapid Communications*.

John Wiley & Sons, Ltd January 1, 2019, p 1800570. DOI:10.1002/marc.201800570.

(11) Feng, X.; Lv, F.; Liu, L.; Tang, H.; Xing, C.; Yang, Q.; Wang, S. Conjugated Polymer Nanoparticles for Drug Delivery and Imaging. *ACS Applied Materials and Interfaces* **2010**, *2* (8), 2429–2435. DOI:10.1021/AM100435K.

(12) Yao, C. J.; Zhang, H. L.; Zhang, Q. Recent Progress in Thermoelectric Materials Based on Conjugated Polymers. *Polymers 2019, Vol. 11, Page 107* **2019**, *11* (1), 107. DOI:10.3390/POLYM11010107.

(13) Wang, S.; Zuo, G.; Kim, J.; Sirringhaus, H. Progress of Conjugated Polymers as Emerging Thermoelectric Materials. *Progress in Polymer Science* **2022**, *129*, 101548. DOI:10.1016/J.PROGPOLYMSCI.2022.101548.

(14) Nguyen, T. N.; Phung, V. D.; Tran, V. Van. Recent Advances in Conjugated Polymer-Based Biosensors for Virus Detection. *Biosensors 2023, Vol. 13, Page 586* **2023**, *13* (6), 586. DOI:10.3390/BIOS13060586.

(15) Müllen, K.; Scherf, U. Conjugated Polymers: Where We Come From, Where We Stand, and Where We Might Go. *Macromolecular Chemistry and Physics*. John Wiley & Sons, Ltd February 1, 2023, p 2200337. DOI:10.1002/macp.202200337.

(16) Swager, T. M. 50th Anniversary Perspective: Conducting/Semiconducting Conjugated Polymers. A Personal Perspective on the Past and the Future. **2017**, *50* (13), 4867–4886. DOI:10.1021/acs.macromol.7b00582.

(17) Hoeben, F. J. M.; Jonkheijm, P.; Meijer, E. W.; Schenning, A. P. H. J. About Supramolecular Assemblies of π-Conjugated Systems. *Chemical Reviews* **2005**, *105* (4), 1491–1546. DOI:10.1021/CR030070Z.

(18) Sirringhaus, H.; Brown, P. J.; Friend, R. H.; Nielsen, M. M.; Bechgaard, K.; Langeveld-

Voss, B. M. W.; Spiering, A. J. H.; Janssen, R. A. J.; Meijer, E. W.; Herwig, P.; De Leeuw, D. M. Two-Dimensional Charge Transport in Self-Organized, High-Mobility Conjugated Polymers. *Nature 1999 401:6754* **1999**, *401* (6754), 685–688. DOI:10.1038/44359.

(19) Noriega, R.; Rivnay, J.; Vandewal, K.; Koch, F. P. V.; Stingelin, N.; Smith, P.; Toney, M. F.; Salleo, A. A General Relationship between Disorder, Aggregation and Charge Transport in Conjugated Polymers. *Nature Materials 2013 12:11* **2013**, *12* (11), 1038–1044. DOI:10.1038/nmat3722.

(20) Park, K. S.; Xue, Z.; Patel, B. B.; An, H.; Kwok, J. J.; Kafle, P.; Chen, Q.; Shukla, D.; Diao, Y. Chiral Emergence in Multistep Hierarchical Assembly of Achiral Conjugated Polymers. *Nature Communications 2022 13:1* **2022**, *13* (1), 1–14. DOI:10.1038/s41467-022-30420-6.

(21) Moris, M.; Van Den Eede, M. P.; Koeckelberghs, G.; Deschaume, O.; Bartic, C.; Van Cleuvenbergen, S.; Clays, K.; Verbiest, T. Harmonic Light Scattering Study Reveals Structured Clusters upon the Supramolecular Aggregation of Regioregular Poly(3-Alkylthiophene). *Communications Chemistry* **2019**, *2* (1), 1–9. DOI:10.1038/s42004-019-0230-4.

(22) Verswyvel, M.; Monnaie, F.; Koeckelberghs, G. AB Block Copoly(3-Alkylthiophenes): Synthesis and Chiroptical Behavior. *Macromolecules* **2011**, *44* (24), 9489–9498. DOI:10.1021/ma2021503.

(23) Timmermans, B.; Koeckelberghs, G. Chiral Expression of Co-Crystallizing Poly(Thiophene)-Block-Poly(Selenophene) Copolymers. *Polymer Chemistry* **2020**, *11* (15), 2715–2723. DOI:10.1039/c9py01775e.

(24) Verheyen, L.; De Winter, J.; Gerbaux, P.; Koeckelberghs, G. Effect of the Nature and the Position of Defects on the Chiral Expression in Poly(3-Alkylthiophene)S. *Macromolecules* **2019**, *52* (22), 8587–8595. DOI:10.1021/acs.macromol.9b01858.

(25) Peeters, H.; Couturon, P.; Vandeleene, S.; Moerman, D.; Leclère, P.; Lazzaroni, R.; Cat, I. De; Feyter, S. De; Koeckelberghs, G. Influence of the Regioregularity on the Chiral Supramolecular Organization of Poly(3-Alkylsulfanylthiophene)S. *RSC Advances* **2013**, *3* (10), 3342–3351. DOI:10.1039/c2ra22731b.

(26) Van, M.-P.; Eede, D.; Bedi, A.; Delabie, J.; De Winter, J.; Gerbaux, P.; Koeckelberghs, G. Polymer Chemistry Rsc.Li/Polymers The Influence of the End-Group on the Chiral Self-Assembly of All-Conjugated Block Copolymers †. *Polym. Chem* **2017**, *8*, 5666. DOI:10.1039/c7py01043e.

(27) Van Oosten, A.; Verduyckt, C.; De Winter, J.; Gerbaux, P.; Koeckelberghs, G. Influence of the Dispersity and Molar Mass Distribution of Conjugated Polymers on the Aggregation Type and Subsequent Chiral Expression. *Soft Matter* **2023**, *19* (21), 3794–3802. DOI:10.1039/D3SM00163F.

(28) Merrifield, R. B. Solid Phase Peptide Synthesis. I. The Synthesis of a Tetrapeptide. *Journal of the American Chemical Society* **1963**, *85* (14), 2149–2154. DOI:10.1021/ja00897a025.

(29) Takizawa, K.; Tang, C.; Hawker, C. J. Molecularly Defined Caprolactone Oligomers and Polymers: Synthesis and Characterization. *Journal of the American Chemical Society* **2008**, *130* (5), 1718–1726. DOI:10.1021/JA077149W/SUPPL_FILE/JA077149W-FILE002.PDF.

(30) Dong, R.; Liu, R.; Gaffney, P. R. J.; Schaepertoens, M.; Marchetti, P.; Williams, C. M.;

Chen, R.; Livingston, A. G. Sequence-Defined Multifunctional Polyethers via Liquid-Phase Synthesis with Molecular Sieving. *Nature Chemistry* **2019**, *11* (2), 136–145. DOI:10.1038/s41557-018-0169-6.

(31) Xu, H.; Ye, S.; Zhao, R.; Seferos, D. S. Homogeneous Synthesis of Monodisperse Sequence-Defined Conjugated Oligomers by Temperature Cycling. *Angewandte Chemie International Edition* **2022**, *61* (39), e202210340. DOI:10.1002/anie.202210340.

(32) Schumm, J. S.; Pearson, D. L.; Tour, J. M. Iterative Divergent/Convergent Approach to Linear Conjugated Oligomers by Successive Doubling of the Molecular Length: A Rapid Route to a 128Å-Long Potential Molecular Wire. *Angewandte Chemie International Edition in English* **1994**, *33* (13), 1360–1363. DOI:10.1002/ANIE.199413601.

(33) Yu, H.; Li, S.; Schwieter, K. E.; Liu, Y.; Sun, B.; Moore, J. S.; Schroeder, C. M. Charge Transport in Sequence-Defined Conjugated Oligomers. *Journal of the American Chemical Society* **2020**, *142* (10), 4852–4861. DOI:10.1021/jacs.0c00043.

(34) Xu, C.; He, C.; Li, N.; Yang, S.; Du, Y.; Matyjaszewski, K.; Pan, X. Regio- and Sequence-Controlled Conjugated Topological Oligomers and Polymers via Boronate-Tag Assisted Solution-Phase Strategy. *Nature Communications* **2021**, *12* (1), 5853. DOI:10.1038/s41467-021-26186-y.

(35) Barnes, J. C.; Ehrlich, D. J. C.; Gao, A. X.; Leibfarth, F. A.; Jiang, Y.; Zhou, E.; Jamison, T. F.; Johnson, J. A. Iterative Exponential Growth of Stereo- and Sequence-Controlled Polymers. *Nature Chemistry 2015 7:10* **2015**, *7* (10), 810–815. DOI:10.1038/nchem.2346.

(36) Espeel, P.; Carrette, L. L. G.; Bury, K.; Capenberghs, S.; Martins, J. C.; Duprez, F. E.; Madder, A. Multifunctionalized Sequence-Defined Oligomers from a Single Building Block. *Angewandte Chemie - International Edition* **2013**, *52* (50), 13261–13264.

DOI:10.1002/anie.201307439.

(37) Zuckermann, R. N.; Kerr, J. M.; Moosf, W. H.; Kent, S. B. H. Efficient Method for the Preparation of Peptoids [Oligo(N-Substituted Glycines)] by Submonomer Solid-Phase Synthesis. *Journal of the American Chemical Society*. American Chemical Society December 1, 1992, pp 10646–10647. DOI:10.1021/ja00052a076.

(38) Porel, M.; Alabi, C. A. Sequence-Defined Polymers via Orthogonal Allyl Acrylamide Building Blocks. *Journal of the American Chemical Society* **2014**, *136* (38), 13162–13165. DOI:10.1021/ja507262t.

(39) Solleder, S. C.; Meier, M. A. R. Sequence Control in Polymer Chemistry through the Passerini Three-Component Reaction. *Angewandte Chemie - International Edition* **2014**, *53* (3), 711–714. DOI:10.1002/anie.201308960.

(40) Pfeifer, S.; Zarafshani, Z.; Badi, N.; Lutz, J. F. Liquid-Phase Synthesis of Block Copolymers Containing Sequence-Ordered Segments. *Journal of the American Chemical Society* **2009**, *131* (26), 9195–9197. DOI:10.1021/ja903635y.

(41) Milis, W.; Peeters, J.; Erkens, R.; De Winter, J.; Gerbaux, P.; Koeckelberghs, G. Versatile Strategy to Develop Sequence-Defined Conjugated Macromolecules: A Powerful Tool toward Tunable Optoelectronic Properties. *ACS Macro Letters* **2024**, 1293–1303. DOI:10.1021/acsmacrolett.4c00526.

(42) Miyaura, N.; Suzuki, A. Palladium-Catalyzed Cross-Coupling Reactions of Organoboron Compounds. *Chemical Reviews* **1995**, *95* (7), 2457–2483. DOI:10.1021/CR00039A007/ASSET/CR00039A007.FP.PNG_V03.

(43) Wadsworth, W. S.; Emmons, W. D. The Utility of Phosphonate Carbanions in Olefin Synthesis. *Journal of the American Chemical Society* **1961**, *83* (7), 1733–1738.

DOI:10.1021/ja01468a042.

(44) Martin, R.; Buchwald, S. L. Palladium-Catalyzed Suzuki-Miyaura Cross-Coupling Reactions Employing Dialkylbiaryl Phosphine Ligands. *Accounts of Chemical Research*. 2008, pp 1461–1473. DOI:10.1021/ar800036s.

(45) Tkachov, R.; Senkovskyy, V.; Komber, H.; Sommer, J.-U.; Kiriy, A. Random Catalyst Walking along Polymerized Poly(3-Hexylthiophene) Chains in Kumada Catalyst-Transfer Polycondensation. *Journal of the American Chemical Society* **2010**, *132* (22), 7803–7810. DOI:10.1021/ja102210r.